Supporting Information

Engineering Selective Pathways for Photocatalytic Methyl Mercaptan Oxidation via Spatially Separated Redox Centers in Sr-Modified Carbon Nitride

*Shanrong Li, Jiali Wang, Shuangqing Liu, Fanghua Zeng, Zhiqi Wen, Rui Xiong, Can Yang**

Characterization

Density functional theory (DFT) calculations were performed using the Perdew–Burke–Ernzerhof (PBE) exchange-correlation functional within the generalized gradient approximation (GGA) (Perdew et al., 1997), as implemented in the Vienna Ab initio Simulation Package (VASP) (Hafner 2008). The interaction between the ionic cores and valence electrons was described using the projector augmented-wave (PAW) method (Blöchl 1994). The long-range van der Waals interactions were taken into account using the Grimme DFT-D3 dispersion correction. Sr doping accompanied by the formation of a neighboring N vacancy was modeled using a 2 × 2 × 1 supercell. The plane-wave cutoff energy was set to 500 eV, and all structures were fully relaxed until the residual forces on each atom were below 0.02 eV Å-1, with the total energy convergence criterion set to 10^{-5} eV. The Brillouin zone was sampled using a 3 ×3 × 1 Monkhorst–Pack k-point mesh. A vacuum layer of at least 25 Å was introduced to eliminate periodic interactions. The measurement work of the scanning electron microscope (SEM) was accomplished by using the Hitachi S4800 electron microscope (employing field emission technology). At the liquid nitrogen temperature (77K), the N_2 adsorption-desorption isotherms were measured using the ASAP 2020 instrument (Mickmoreitik Instruments Company, USA). The specific surface area was calculated by the Brunauer-Emmett-Teller (BET) method. The UV-vis diffuse reflection spectrascopy (DRS) were performed on a Varian Cary 500 Scan UV-vis system. The photoelectric current performance and impedance tests were conducted in a traditional three-electrode battery using the BAS Epsilon electrochemical system. Platinum plate was used as the reference electrode, and the Ag/AgCl (3 M KCl) electrode was used as the reference electrode. The working electrode was fabricated on fluorine-tin oxide glass, with a working area of approximately 0.3 cm^2. The electrolyte was a 0.2 M sodium sulfate aqueous solution (pH = 6.8). Visible light was provided by a 300 W xenon lamp, with a cutoff filter for wavelengths > 420 nm. The bias potential was set at -0.2 volts relative to Ag/AgCl, in the mechanism

exploration experiment, the establishment of a special atmosphere test environment was achieved by controlling the flow rate of the required gas to be 10 ml min^{-1} and introducing it into the electrolyte.

Results and Discussion

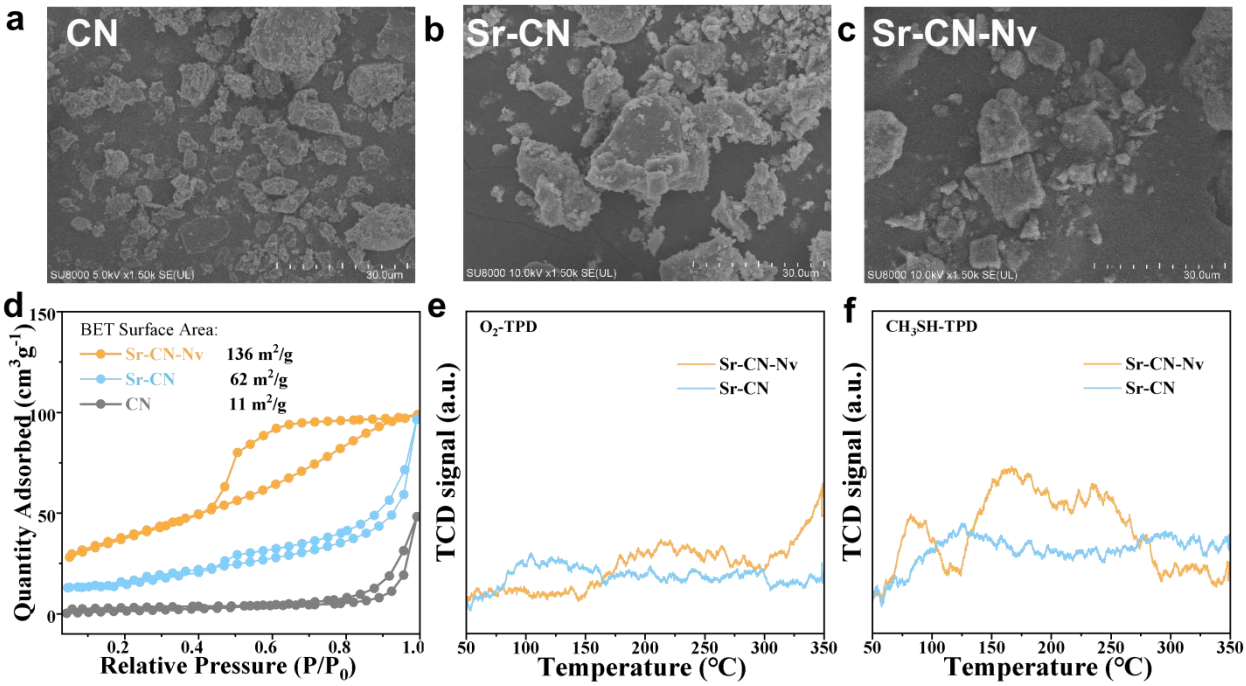

Figure S1. SEM images of a) CN; b) Sr-CN; c) Sr-CN-Nv, d) N_2 adsorption-desorption isotherms of samples, e) O_2-TPD; f) CH_3SH-TPD of Sr-CN and Sr-CN-Nv.

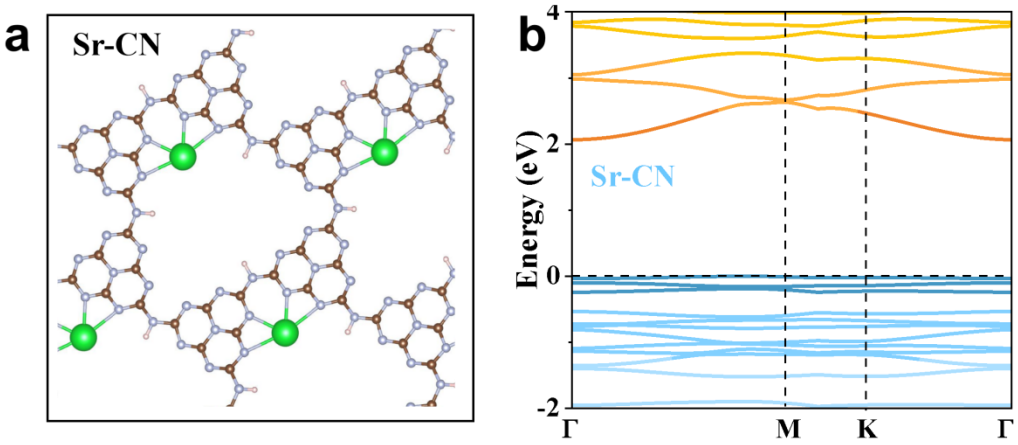

Figure S2. a) Structural models and b) Calculated band structures of Sr-CN.

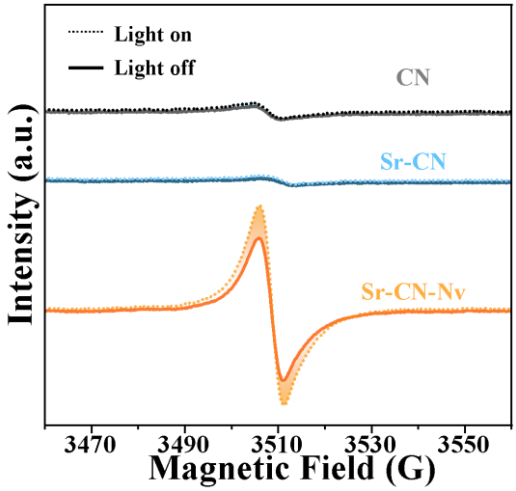

Figure S3. EPR spectrum of CN, Sr-CN and Sr-CN-Nv.

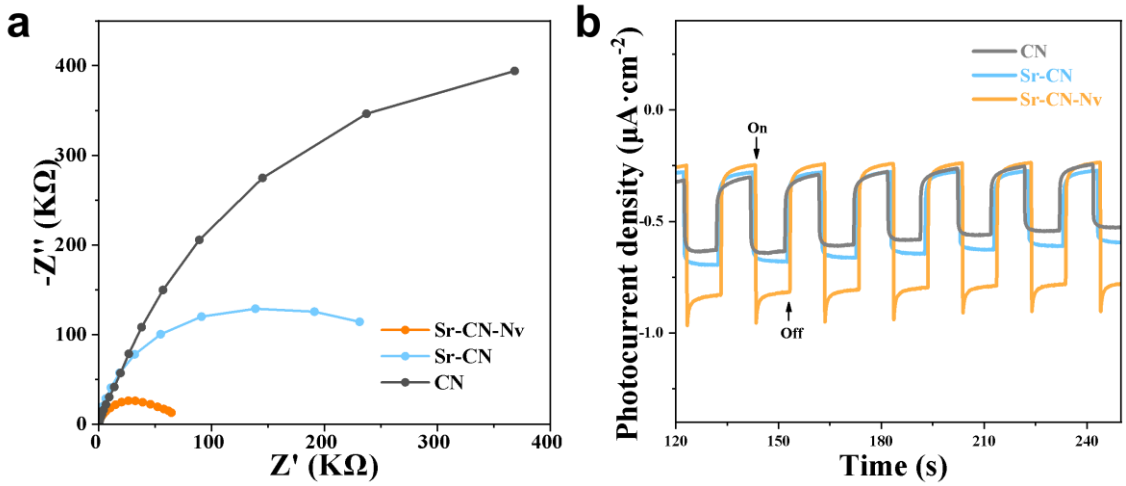

Figure S4. a) EIS spectra and b) Transient photocurrent responses (-0.2 V vs. Ag/AgCl, pH 6.8) of CN, Sr-CN and Sr-CN-Nv.

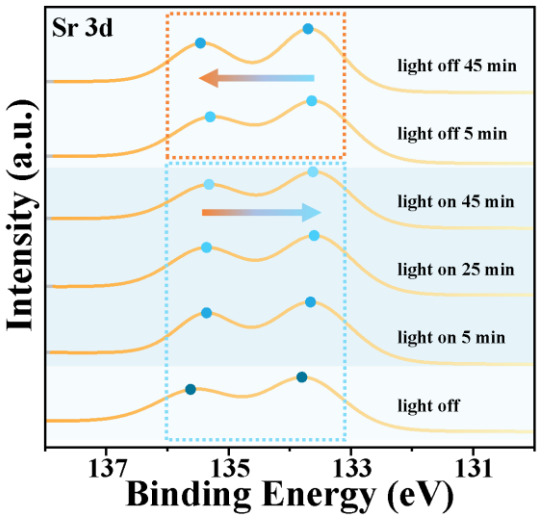

Figure S5. The fitting results of the XPS-Sr 3d spectra that vary with light exposure time

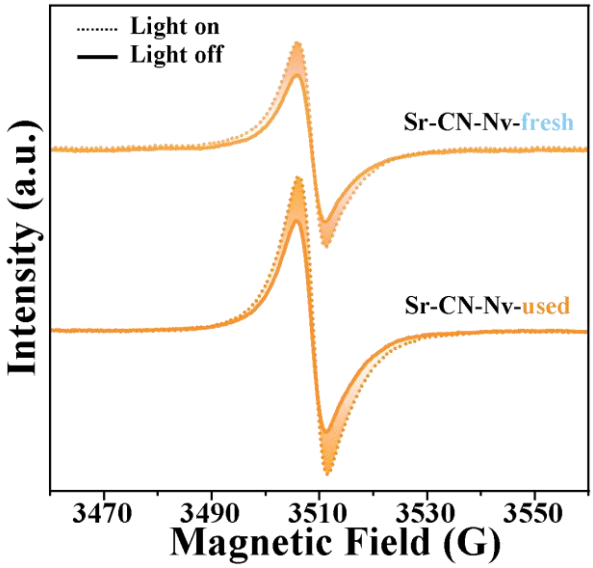

Figure S6. EPR spectrum of Sr-CN-Nv before and used.

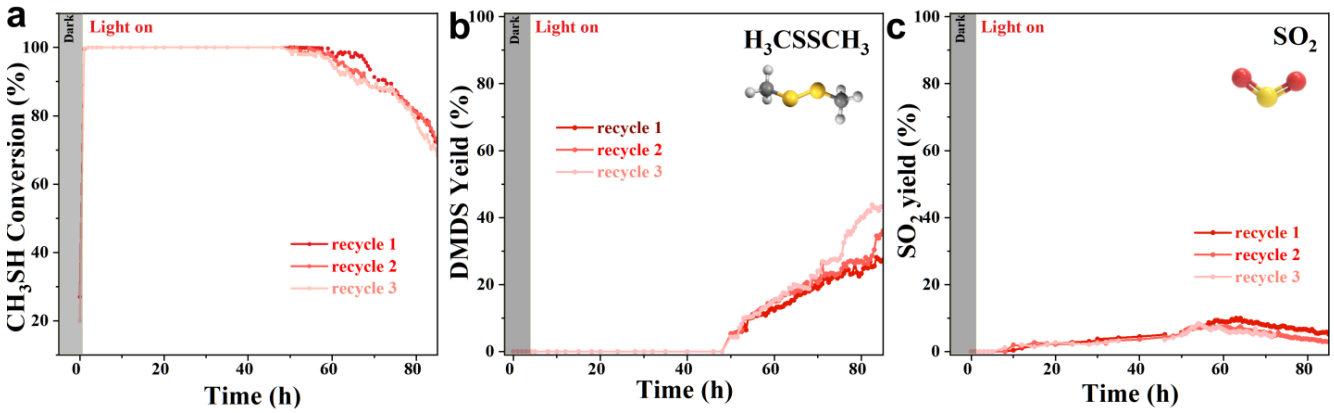

Figure S7. Stability tests of the Sr-CN-Nv for 3 cycles. Photocatalytic degradation of CH_3SH (condition: catalyst mass 40 mg, 100 ppm CH_3SH with N_2 balance, 5% O_2, total flow rate = 10 mL·min^{-1}, reaction temperature: 40 °C, 420 nm LED (50 W)): a) CH_3SH Conversion; b) DMDS yield; c) SO_2 Yield.

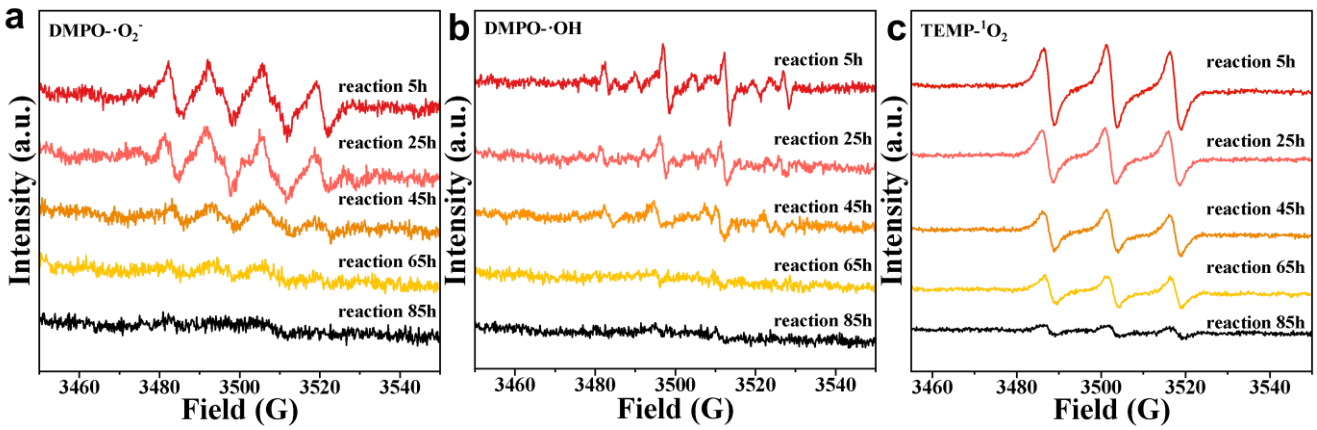

Figure S8. EPR spectra of reactive oxygen species in samples collected at different stages of the reaction: (a) superoxide radical, (b) hydroxyl radical, (c) singlet oxygen.

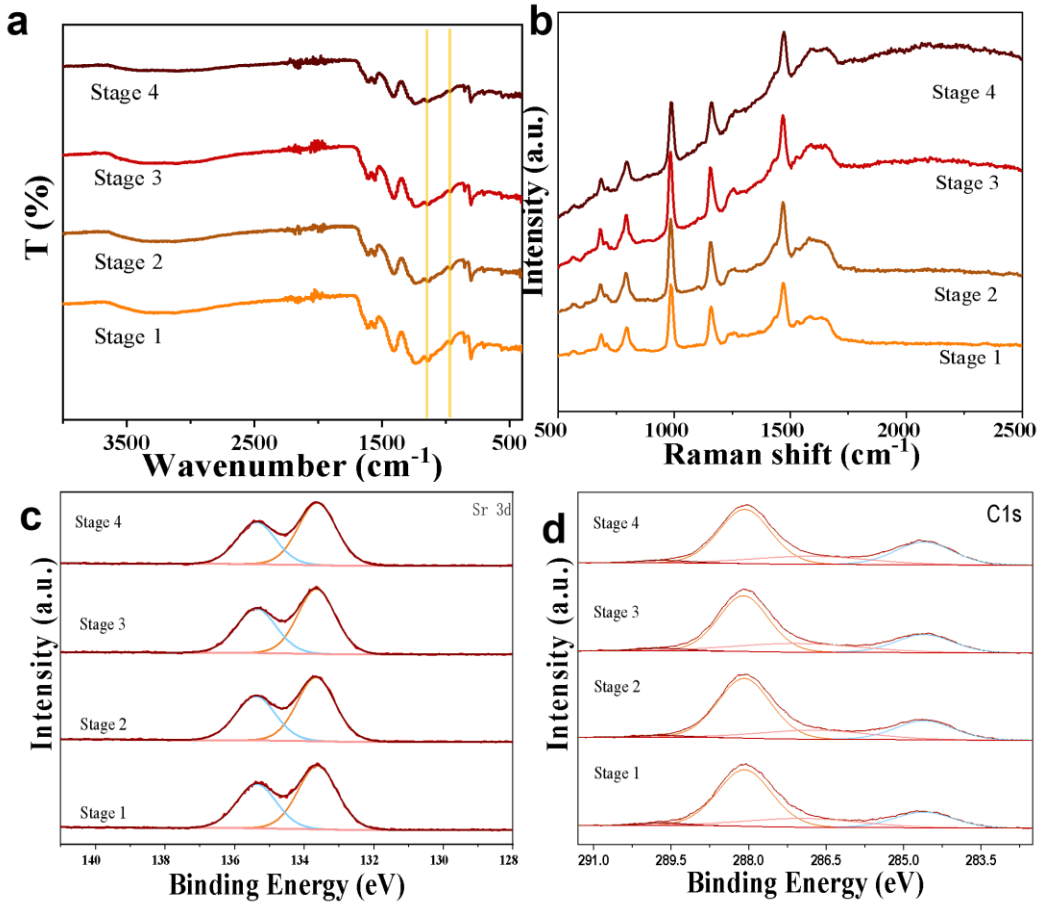

Figure S9. a) FT-IR spectra, b) Raman spectra, c) XPS-Sr 3d spectra, d)XPS-C1s spectra of Sr-CN-Nv in different reaction stage.

Table S1 Exafs analysis fitting parameters

Sample	Path	coordination number	R(Å)	ϭ2(Å2)	ΔE（ev)	R factor
Sr foil	Sr-Sr	12				
SrO	Sr-O	3	2.55±0.02	0.010	-4.102±2.3	0.020
	Sr-Sr	12	4.19±0.01	0.002		
Sr-1	Sr-O/N	4.640	2.59±0.03	0.012	5.812±1.69	0.013
Sr-2	Sr-O/N	5.095	2.78±0.02	0.017	6.759±1.39	0.015

REFERENCES

Perdew, J. P.; Burke, K.; Ernzerhof, M (1997) Generalized Gradient Approximation Made Simple. Physical Review Letters. 78: 1396-1396

Hafner, J (2008) Ab-initio Simulations of Materials using VASP: Density-functional Theory and Beyond. Journal of Computational Chemistry. 29: 2044-2078

Blöchl, P. E (1994) Projector Augmented-wave Method. Physical. Review. B 50: 17953-17979